Excited-State Deactivation Mechanisms of the $M_2(dba)_3$ Complexes (M = Pd(0), Pt(0); dba = Dibenzylideneacetone)

Stephan M. Hubig,*,† Marc Drouin,‡ André Michel,‡,§ and Pierre D. Harvey*,‡

Center for Fast Kinetics Research University of Texas at Austin, Austin, Texas 78712, and Département de Chimie, Université de Sherbrooke, Sherbrooke, PQ, Canada J1K 2R1

Received February 19, 1992

The flash photolysis transients (30 ps–10 μs) of the $M_2(dba)_3$ complexes (M = Pd, Pt; dba = dibenzylideneacetone) have been investigated in toluene solutions at 298 K. Due to the biphasic decay kinetic results observed in the $Pd_2(dba)_3$ case, the flash photolysis experiments were also performed on the free dba ligand and two substituted derivatives (bis(2-methylbenzylidene)acetone (Medba) and bis(2-methoxybenzylidene)acetone (MeOdba)). For the free ligands, two transient species are observed, a short-lived one ($8.3 < \tau < 13.3$ ns; broad band located at ~470 nm) corresponding to the intraligand triplet excited state and a longer-lived one (2.5–6.4 μs; narrower band located at ~450 nm) associated with the geometric isomers responsible for the cis,trans-isomerization reactions. On the other hand, $M_2(dba)_3$ difference absorption spectra (M = Pd, Pt) exhibit intense transient signals located at ~600 and ~660 nm for M = Pd and Pt, respectively, which decay via a double exponential for M = Pd (1.0 ns and 0.50 μs) and a single exponential for M = Pt (0.26 μs). The μs values are the metal-to-ligand charge-transfer (MLCT) triplet excited-state lifetimes, and the ns value is assigned to a new species associated with a geometric isomer photoinduced by a labile dba ligand. Qualitative MO analysis (extended Hückel calculations) on free dba in its s-cis,s-cis and s-cis,s-trans conformations and on the model compounds $Pd_2(CH_2{=}CH(CO)CH{=}CH_2)_3$ and $Pd_2(dba)(CH_2{=}CH(CO)CH{=}CH_2)_2$ have confirmed the intraligand charge-transfer states (ILCT) for dba and the metal-to-ligand charge-transfer (MLCT) states for the $M_2(dba)_3$ complexes. More importantly, the LUMO's for dba and $Pd_2(dba)(CH_2{=}CH(CO)CH{=}CH_2)_2$ have very similar atomic contributions and would suggest that excited-state deactivations for dba and $M_2(dba)_3$ (M = Pd, Pt) could indeed follow similar processes. Finally, the Medba has been characterized by single-crystal X-ray diffraction (for EHMO calculation purposes) and adopts the s-cis,s-cis configuration, where the methyl groups (2-positions) are oriented parallel with the carbonyl group. X-ray data: orthorhombic space group *Pcab*, $a = 8.6846$ (9) Å, $b = 13.8279$ (9) Å, $c = 25.664$ (3) Å, $V = 3082.0$ (5) Å^3, $Z = 8$, 1993 unique reflections, $R = 0.071$, and $R_w = 0.054$.

Introduction

The electron-rich d^{10}–d^{10} M_2 complexes (M = Pd(0), Pt(0), Ag(I), Au(I)) have been proposed as good candidates for photocatalysis.[1] Such complexes are luminescent in fluid solutions at 298 K and exhibit relatively long-lived excited states (0.2–6.0 μs).[2-6] On some occasions efficient photoinduced oxidative addition reactions have been observed.[1] Important exceptions are the air-stable $M_2(dba)_3$ complexes (M = Pd, Pt; dba = dibenzylideneacetone), where the excited-state redox potentials for the lowest energy excited states (MLCT; metal-to-ligand charge transfer)[2,3] are relatively small ($E^{\circ +/*}(^3MLCT^*) = -0.33$ V vs SSCE for both M = Pd and Pt)[7,8] and appear to be photochemically inert toward oxidative additions in the presence of chlorinated hydrocarbons (CH_2Cl_2, $CHCl_3$, $ClCH_2CH_2Cl$) and molecular oxygen.[7,8] This behavior could be a reflection of the better π-acceptor properties of the dba ligand over the commonly investigated phosphines. One further interesting difference between the $M_2(dba)_3$ and other M_2 d^{10}–d^{10} complexes is that the colored dba ligand exhibits relatively low energy[7,8] excited states that lie nearby the M_2 ones[2-4] and could participate in the photochemistry of the dimers. One other distinguishing characteristic is that dba may exist into two experimentally observed geometric forms, s-cis,s-cis and s-cis,s-trans, in the free and complexed states.[9-12]

In this paper we will present the flash photolysis studies (30 ps–10 μs) and the kinetic data associated with the transient and excited-state deactivation for the $M_2(dba)_3$ complexes (M = Pd, Pt). During the course of our investigations, we have noticed that the excited $Pd_2(dba)_3$ deactivation showed biphasic decay kinetics which led us to investigate the photophysics of three free ligands (dba, MeOdba, Medba). Lifetimes for triplet excited states and geometric isomers have been measured, and it will be suggested that the transient species observed for the free ligands are somewhat similar to the short-lived one for the $Pd_2(dba)_3$ compound indicating that the dba ligand contributed efficiently to the excited-state deactivation in this complex. Since the $M_2(dba)_3$ complexes (M = Pd, Pt) are luminescent in solution, a qualitative molecular orbital study (extended Hückel calculations) of the model compounds $Pd_2(CH_2{=}CH(CO)CH{=}CH_2)_3$ and $Pd_2(dba)(CH_2{=}CH(CO)CH{=}CH_2)_2$, where the ligands are in the s-cis,s-trans conformation (C_3 point group when ignoring the phenyl groups), was undertaken to determine the nature of the

* To whom correspondence should be addressed.
† University of Texas at Austin.
‡ Université de Sherbrooke.
§ Correspondence pertaining to the crystallographic results should be addressed to this author.

(1) Caspar, J. V. *J. Am. Chem. Soc.* **1985**, *107*, 6718.
(2) Kane-Maguire, N. A. P.; Wright, L. L.; Guckert, J. A.; Tweet, W. S. *Inorg. Chem.* **1988**, *27*, 2905.
(3) (a) Harvey, P. D.; Adar, F.; Gray, H. B. *J. Am. Chem. Soc.* **1989**, *111*, 1312. (b) Harvey, P. D.; Gray, H. B. *Polyhedron* **1990**, *9*, 1949. (c) Harvey, P. D.; Gan, L. *Inorg. Chem.* **1991**, *30*, 3239.
(4) Harvey, P. D.; Gray, H. B. *J. Am. Chem. Soc.* **1988**, *110*, 4391.
(5) Che, C.-M.; Wong, W. T.; Lai, T.-F.; Kwong, H.-L. *J. Chem. Soc., Chem. Commun.* **1989**, 243.
(6) King, C.; Wang, J.-C.; Khan, Md. N. I.; Fackler, J. P., Jr. *Inorg. Chem.* **1989**, *28*, 2145.
(7) Harvey, P. D.; Gan, L.; Aubry, C. *Can. J. Chem.* **1990**, *68*, 2278.
(8) Harvey, P. D.; Aubry, C.; Gan, L.; Drouin, M. *J. Photochem. Photobiol. A: Chem.* **1991**, *57*, 465.
(9) Mazza, M. C.; Pierpont, C. G. *J. Chem. Soc., Chem. Commun.* **1973**, 207.
(10) Ukai, T.; Kawazura, H.; Ishii, Y.; Bonnet, J. J.; Ibers, J. A. *Organomet. Chem.* **1974**, *65*, 253.
(11) Tanaka, H.; Kawazura, H. *Bull. Chem. Soc. Jpn.* **1979**, *52*, 2815.
(12) Tanaka, H.; Kawazura, H. *Bull. Chem. Soc. Jpn.* **1980**, *53*, 1743.

0020-1669/92/1331-5375$03.00/0

orbitals involved, particularly for the HOMO and LUMO. It will be shown for the first time that the LUMO's for the dba ligand and the model compound $Pd_2(dba)(CH_2{=}CH(CO)CH{=}CH_2)_2$ are essentially the same. During the course of our work, the crystal and molecular structures of Medba have also been determined by single-crystal X-ray crystallography in order to obtain structural data for the free ligands in the EHMO calculations.

Experimental Section

Materials. Dba, Medba, and MeOdba were synthesized according to a modified procedure reported by Conrad and Doliver.[13] A 2:1 corresponding aldehyde–acetone mixture was added dropwise (~1 drop/s) to the 10% NaOH water–ethanol (1:1) solution. The corresponding aldehydes, 2-methylbenzaldehyde and 2-methoxybenzaldehyde (Aldrich Chemical Co.), were used as received. For the solid aldehyde, a saturated ethanol solution was made prior to addition. After the solution was stirred for 2 h, an equivalent portion of water was slowly added to complete precipitation of the yellow product. After filtration, the filtrate was dried in vacuo (10^{-6} Torr; 24 h). The compounds were characterized by ^{1}H-NMR, UV–vis, and IR spectroscopy and elemental analysis. Crystals suitable for X-ray analysis were obtained by slow evaporation of a concentrated solution of Medba in a toluene–propanol mixture. The $M_2(dba)_3$ complexes were synthesized according to standard procedures (M = Pd,[14] Pt[15]). The complexes were purified by recrystallization in dry chloroform/hexane. Purity was checked by elemental analysis and ^{1}H-NMR spectroscopy. Toluene (B&J) was purified by fractional distillation and dried over Na(s) until the solvent made a clear glass at 77 K or was from Aldrich Chemical Co. as HPLC grade/glass distilled (99.9%+).

All spectroscopic measurements were performed immediately after N_2(g)-bubbling degassing of the solutions, unless stated otherwise.

Spectroscopic Measurements. The absorption spectra were measured on a Hewlett Packard 8452 A diode array spectrophotometer. The emission and excitation spectra were obtained using a Spex Fluorolog II spectrometer. The phosphorescence spectra and lifetime measurements were performed on a Spex 1934D phosphorimeter coupled with the Spex Fluorolog spectrometer.

Picosecond Time-Resolved Measurements. The laser source for the picosecond time-resolved kinetic measurements was a mode-locked Nd:YAG laser (Quantel YG 402). Both the harmonic (532 or 355 nm) and the residual 1064-nm light pulses were extracted from the laser and traveled together to a dichroic mirror that reflected the harmonic laser pulse in a 90° angle and transmitted the 1064-nm light. While the harmonic light was focused onto the sample cuvette, the 1064-nm light traversed a variable delay stage before being focused onto a 10-cm cuvette containing a 50:50 mixture of deuterated phosphoric acid and D_2O to produce a white continuum light flash of 30-ps duration. The continuum light was focused through a diffusing frosted glass plate and recollimated and focused onto the common end of a bifurcated fiber optics bundle that split the beam into two branches, a sample beam that probed the sample where it was excited by the harmonic laser pulse (excited state) and a reference beam that probed the sample where it was not excited (ground state). The two light beams were picked up by fiber optics on the other side of the cuvette and led to a UFS 200 spectrograph to which a dual diode array (2 × 512) with image intensifier was attached. Thus, with one single continuum flash the spectra of excited and unexcited sample could be detected. The wavelength resolution of the system was 1 nm per diode. The diode array data were passed via a Tracor Northern 6200 multichannel analyzer to a personal computer for storage, analysis, and display. In a typical experiment about 200 spectra were averaged from one delay time. When the delay stage was moved, the arrival of the continuum flash could be delayed by up to 5 ns with respect to the excitation pulse generating time-resolved spectra with a time resolution limited only by the pulse width of the laser (ca. 30 ps). Before each measurement the two diode arrays were balanced and all reference beam data were corrected by this balance factor before calculating the difference absorption of the transient species for each wavelength: $A = \log(I(\text{reference})/I(\text{sample}))$.

Table I. X-ray Diffraction Acquisition Parameters

formula	$C_{19}H_{18}O_1$
fw	262.35
space gp	*Pcab*
a, Å	8.6846 (9)
b, Å	13.8279 (9)
c, Å	25.664 (3)
V, Å^3	3082.0 (5)
Z	8
d_{calc}, Mg m^{-3}	1.131
cryst dimens, mm	0.2 × 0.2 × 0.3
temp, K	293
radiation, Å	0.710 73 (Mo K$\bar{\alpha}$)
monochromator	graphite
linear abs coeff, cm^{-1}	0.63
diffractometer	Enraf-Nonius CAD-4
scan method	$\omega/2\theta$
h,*k*,*l* limits	0/8; 0/14; 0/27
2θ range, deg	$2.0 \le 2\theta \le 44.9$
scan width, deg	0.8°
program used	NRCVAX
F(000)	1119.87
weighting	counting statistics
no. of unique data	1993
data with $I \ge 2.0\sigma(I)$	990
no. of variables	254
largest shift/esd in final cycle	0.031
R	0.071
R_w	0.054
goodness of fit	1.94
secondary extinction coeff	0.36 (7)

Nanosecond and Microsecond Time-Resolved Measurements. The nanosecond and microsecond time-resolved kinetic measurements were performed using a Q-switched Nd:YAG laser (Quantel YG 581) with a ca. 10-ns pulse and a kinetic spectrophotometer including an Oriel 150-W xenon lamp, a computer-driven Spex monochromator, and a Hamamatsu R928 photomultiplier tube. The data were collected by either a Tektronix 7912 digitizer (for nanosecond time scales) or a Biomation 8100 digitizer (for microsecond time resolution) and stored in a personal computer for kinetic analysis. All samples were deaerated prior to laser flash photolysis by bubbling with nitrogen gas.

Crystallography. A single crystal was mounted on an Enraf-Nonius CAD-4 diffractometer using monochromatized Mo Kα radiation (λ = 0.710 73 Å) at a constant speed of 2.7° min^{-1} with an $\omega/2\theta$ scan. Two standard reflections were remeasured every 60 min, showing no significant decay. The lattice parameters were refined from 24 reflections with 2θ range 30–40°. Intensities were corrected for Lorentz and polarization effects. A total of 1993 unique reflections were measured where 990 were observed with $I_{net} \ge 1.8\sigma(I_{net})$. The NRCVAX system[16] was used for all calculations; these were done on an IBM RISC/6000 computer. The structure was solved using direct methods. All non-H atoms were refined anisotropically. All hydrogen positions were calculated and refined. The final residuals at convergence were $R = 0.071$, $R_W = 0.054$, and $S = 1.94$; $(\Delta/\sigma \text{ max}) = 0.031$, and the secondary extinction coefficient[17,18] was 0.36 (7). Weights based on counting statistics were used. The maximum and minimum density peaks in the final difference Fourier map were respectively 0.30 and –0.24 e Å^{-3}. Scattering factors were taken from ref 19. The acquisition parameters are listed in Table I.

Computational Details. All of the MO calculations were of the extended Hückel type (EHMO)[20-22] using a modified version of the Wolfsberg–Helmholz formula.[23] The atomic parameters used for C, O, and H are

(13) Conrad, C. R.; Dolliver, M. A. *Organic Synthesis, Collection*; John Wiley: New York, 1943; Vol. 2, p 167.
(14) Takahashi, Y.; Ito, T.; Ishii, Y. *J. Chem. Soc., Chem. Commun.* **1970**, 1065.
(15) Moseley, K.; Maitlis, P. M. *J. Chem. Soc., Chem. Commun.* **1971**, 982.
(16) Gabe, E. J.; Lee, F. L.; LePage, Y. *Crystallographic Computing: Data Collection, Structure Determination, Proteins and Databases*; Sheldrick, G. M., Krüger, C., Godalard, R., Eds.; Clarendon Press: Oxford, U.K., 1985; pp 167–174.
(17) Larson, A. C. *Acta Crystallogr.* **1967**, *23*, 664.
(18) Zachariasen, W. H. *Acta Crystallogr.* **1963**, *16*, 1139.
(19) Cromer, D. T.; Waber, J. T. *International Tables for X-Ray Crystallography*; Ibers, J. A., Hamilton, W. C., Eds.; Kynoch Press: Birmingham, U.K., 1974; Vol. IV, Table 2.2B, pp 99–101 (present distribution Kluwer Academic Publischer, Dordrecht, The Netherlands).
(20) Hoffmann, R.; Lipscomb, W. N. *J. Chem. Phys.* **1962**, *36*, 2179.
(21) Hoffmann, R.; Lipscomb, W. N. *J. Chem. Phys.* **1962**, *37*, 2872.
(22) Hoffmann R. *J. Chem. Phys.* **1963**, *39*, 1397.
(23) Ammeter, J. H.; Burgi, H. B.; Thibeault, J. C.; Hoffmann, R. *J. Am. Chem. Soc.* **1978**, *100*, 3686.

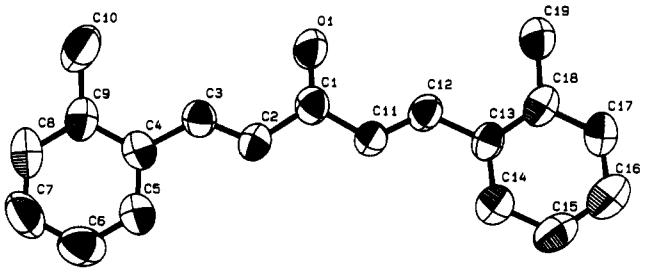

Figure 1. ORTEP drawing for Medba showing 50% of thermal ellipsoids and atom numbering for the X-ray data. The H-atoms have not been drawn on this picture. Selected data are as follows. Bond distances (Å): C1–O1 = 1.231 (6); C1–C2 = 1.461 (7); C2–C3 = 1.308 (7); C3–C4 = 1.467 (7). The torsional angle between the C2–C3–C4 plane and C3–C4–C9 is 167.6 (9)°, while the others approach 180° within ~3°.

taken from refs 20–22; those for the Pd atoms are taken from ref 24. The $Pd_2(dba)_3 \cdot CH_2Cl_2$ crystal structure data were used,[25] where the C–O, C–H, C=C, C–C, and Pd–C distances were fixed at 1.26, 1.05, 1.35, 1.50, and 2.26 Å, respectively. The detailed description for the graphic programs used in this work can be found in ref 26. Solution NMR studies proved that $Pd_2(dba)_3$ has the same structure in solution as in the solid state.[27]

Results and Discussion

X-ray Structure. Medba crystallizes in a quasi-planar s-cis,s-cis configuration (Figure 1) with the methyl groups being oriented parallelly with the ketone. The torsional angle between the C2–C3–C4 and C3–C4–C9 planes (or the phenyl plane) is 167.6 (9)°, while the other torsional angles approach 180 ± 3°, and is presumably due to crystal packing. The C–C and C–O bond distances and C–C–C and C–C–O angles are all normal. A previous X-ray study on dba revealed that free dba also adopts the s-cis,s-cis conformation, but the quality of the crystal prevented the evaluation of accurate bond distances and angles.[8] To our knowledge there is no other crystallographic report on this type of ligand in the uncomplexed state. As expected, we observe some bond length changes (up to 0.04 Å) between the complexed[25] and free ligands (see selected data in Figure 1).

Excited-State Energy Levels. The $Pd_2(dba)_3$ absorption spectra were interpreted previously[2,3] and exhibit electronic bands at ~350, 380, and 545 nm. They are assigned to intraligand charge-transfer (ILCT),[7] $d\sigma^*$–$p\sigma$, and MLCT transitions,[2,3] respectively. An ^{3}MLCT* emission at ~730 nm is also observed. The ILCT, $d\sigma^*$-$p\sigma$, and MLCT* absorption and ^{3}MLCT* emission bands for $Pt_2(dba)_3$ are located at 350, 400, 620, and 800 nm, respectively.[3]

The 77 K phosphorescence spectra for free dba (Figure 2) exhibit a poorly vibronically structured emission located in the 500–700-nm range where the 0–0 transition is depicted at ~550 nm. The emission lifetime is 20 ± 2 μs and compares favorably with that reported for 298 K solid samples (i.e. s-cis,s-cis conformer), via delayed fluorescence spectroscopy (τ_e = 28.5 μs).[9-12] Despite the poor resolution of the spectra, the energy gaps between the vibrational bands are ~1250 cm^{-1} and cannot be assigned to a ν(C=O) mode but rather compared with the one reported for the fluorescence spectra (1260 ± 100 cm^{-1}). This phosphorescence is also preferably assigned to an ILCT emission.

Assuming that the singlet–triplet energy gap for the $^1(d\sigma^*)^1$-$(p\sigma)^*$ excited states is the same (~8200 cm^{-1}) for the isoelectronic $M_2(dba)_3$ and $M_2(dppm)_3$ complexes (M = Pd, Pt; dppm = bis-(diphenylphosphino)methane)[4] and that the triplet ILCT energy for both free and complexed dba is the same, an energy diagram may now be sketched (Scheme I).

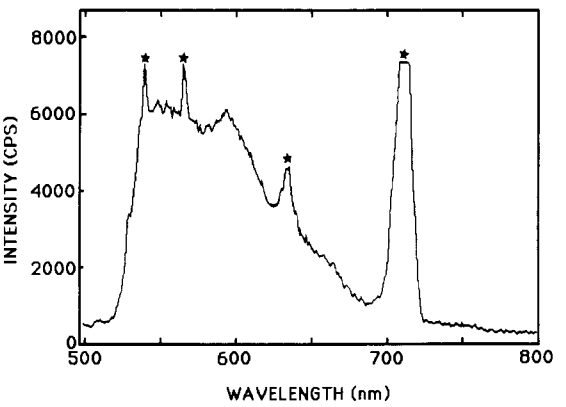

Figure 2. Phosphorescence spectrum of dba in toluene at 77 K. The peaks labeled with stars are instrumental artifacts. The strong peak at 710 nm is the first harmonic of the excitation wavelength (355 nm).

Scheme I

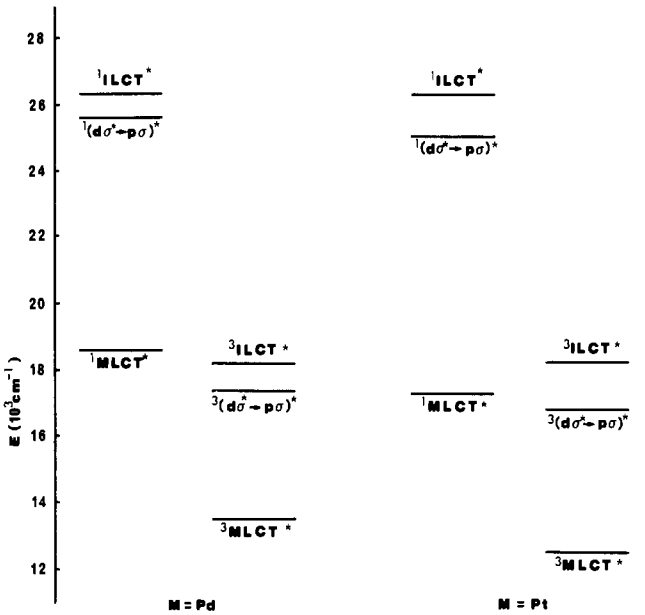

Transient Spectra. The dba flash photolysis spectra upon 355-nm excitation (Figure 3) exhibit bleaching (375 nm) associated with the ILCT band and a broad unresolved transient located at ~470 nm. Both transient and bleached ILCT bands (rise time < 30 ps) decay with the same double kinetics with a short (8.3 ± 1.5 ns) and a long component (5.2 ± 0.1 μs). The absorption band becomes somewhat sharper and moves to ~450 nm at longer delay time. The measured kinetic parameters cannot be attributed to singlet lifetimes by comparison with the ones measured by fluorescence spectroscopy.[7,8]

The lifetime of the longer-lived transient was observed to be independent of the oxygen concentration in the solution. We also noticed a strong temperature dependence of the decay rate constant leading to an activation energy of 10 kcal/mol (see Table II). Moreover, the lifetime did not change with varying magnetic field up to 1200 G. On the basis of these experimental facts, we conclude that this transient cannot be the triplet state as suggested by Temply et al.[28] With an activation energy similar to the one of the trans → cis isomerization of stilbene,[29] we assign this transient to a geometric (cis) isomer of the ground state of dba. To test this hypothesis, flash photolysis experiments on two dba derivatives, 2,2′-dimethyl and 2,2′-dimethoxy dba were performed. However, there is no clear trend in the data (see Table II). This

(24) Tatsumi, K.; Hoffmann, R.; Yamamoto, A.; Stille, J. K. *Bull. Chem. Soc. Jpn.* **1981**, *54*, 1857.
(25) Pierpont, C. G.; Mazza, M. C. *Inorg. Chem.* **1974**, *13*, 1891.
(26) Mealli, C.; Proserpio, D. M. *J. Chem. Educ.* **1990**, *67*, 399.
(27) Kawazura, H.; Tanaka, H.; Yamada, K.; Takahashi, Y.; Ishii, Y. *Bull. Chem. Soc. Jpn.* **1978**, *51*, 3466.
(28) Teply, J.; Bursik, J. *Radioanal. Nucl. Chem.* **1986**, *101*, 369–375.
(29) Saltiel, J.; Sun, Y.-P. In *Photochromism*; Duerr, H., Ed.; Elsevier: Amsterdam, 1990; pp 64–164.

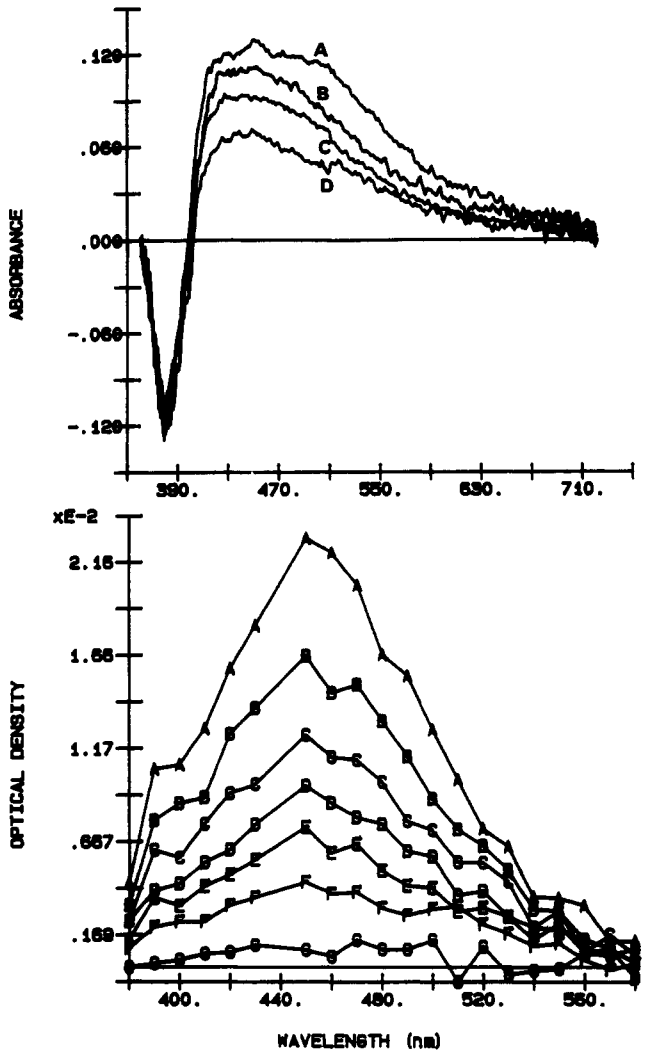

Figure 3. Difference absorption spectra of dba in toluene at various delay times: (top) A = 60 ps, B = 720 ps, C = 2.7 ns, D = 4.7 ns; (bottom) A = 1.2 μs, B = 2.4 μs, C = 3.6 μs, D = 4.8 μs, E = 60 μs, F = 7.8 μs, G = 15.0 μs, using the 355-nm excitation.

Table II. Temperature Dependence of dba Transient Lifetimes

	transient lifetimes, μs			
	dba			
T, °C			Medba	MeOdba
21	5.2[a]	3.5[b]	6.4[a]	2.5[a]
30	2.6	2.2	4.2	1.8
40	1.7	1.7	2.8	1.0
50	1.1	1.0	1.8	0.7
E_A, kcal/mol	10.0	8.1	8.4	8.8

[a] In toluene. [b] In acetonitrile.

can be explained by considering two counteracting effects: steric hindrance of bulky substituents and inductive effects of electron-donating substituents. On the one hand, the lifetime of the isomer is expected to increase with increasing size of the substituents. On the other hand, the electron-donating character of the dimethyl and the dimethoxy substituents stabilizes a partial zwitterionic character of the dba ground state (negative charge on the carbonyl group and positive charge on the phenyl ring), which facilitates rotation around the C,C double bond. This argument is supported by the fact that the lifetimes were shortened in a polar solvent such as acetonitrile (see Table II).

The shorter lived transients (8–13 ns), which also varied with the phenyl substituents, are assigned to triplet states. The very fast decay of the triplet state in solution at room temperature can be explained if we assume that one decay path of the triplet state is to form the isomer of the ground state. Since this isomerization

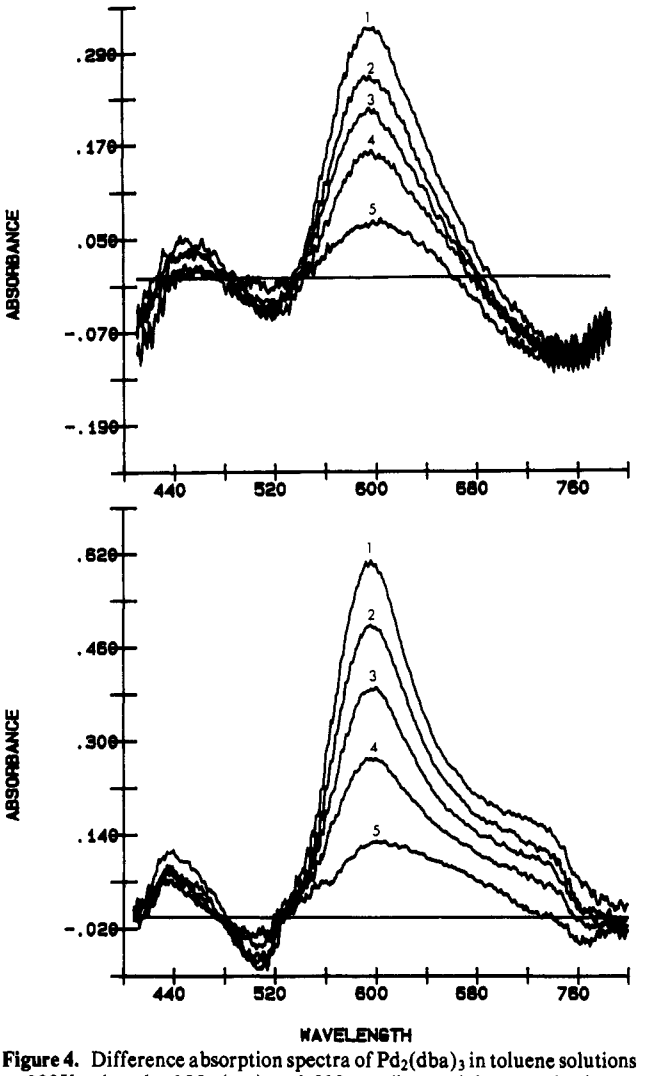

Figure 4. Difference absorption spectra of $Pd_2(dba)_3$ in toluene solutions at 298K using the 355- (top) and 532-nm (bottom) laser excitation at various delay times. Top spectra: 1 = 140 ps, 2 = 470 ps, 3 = 800 ps, 4 = 1.1 ns, 5 = 4.8 ns; bottom: 1 = 140 ps, 2 = 470 ps, 3 = 800 ps, 4 = 1.5 ns, 5 = 4.8 ns.

is hindered in the solid state as well as in frozen solvents (77 K), we obtained much longer triplet lifetimes under those conditions.

The $Pd_2(dba)_3$ difference absorption spectra (298 K) are characterized by an intense transient localized at 600 nm which is associated with species that are formed within the 30-ps excitation pulses (Figure 4). Using the 355- and 532-nm excitation lines, the measured spectra are similar, but one difference is noticed. The 730-nm feature (355-nm spectra), which is due to the complex luminescence, is absent from the 532-nm ones and allows the observation of one extra feature (shoulder) located at approximately 710 nm. This new 710-nm feature exhibits the same kinetics as for the 600-nm transient and should be associated with the same species. The lack of observed luminescence in the 532-nm spectra remains unexplained at this stage.

The luminescence decay (750 nm) appears as a single exponential leading to a triplet-state lifetime of 0.53 ± 0.02 μs and is different from the ones measured previously in Me-THF (τ_e = 0.22 ± 0.01 μs).[2,3] On the other hand, the transient (600 and 710) and bleached MLCT bands (520 nm) exhibit a double-exponential deactivation process for both the 355- and 532-nm excitations with an approximate 1:1 intensity ratio. The observed lifetimes are 1.0 ± 0.1 ns and 0.50 ± 0.03 μs. Again there are very little spectroscopic changes with delay times; the longer lifetime was oxygen sensitive and indeed corresponds to the MLCT triplet-state lifetime by comparison with the luminescence lifetime. The 1-ns value is too great to be associated with the $Pd_2(dba)_3$

Table III. Kinetic Data for the Investigated Compounds (298 K)

	dba	Medba	MeOdba	$Pd_2(dba)_3$	$Pt_2(dba)_3$
raise time, ps	<30	<30	<30	<30	<30[b]
short component, ns ● 10%	8.3	8.4	13.3	1.0	[a]
long component, μs (at 21 °C)	5.2 ± 0.1	6.4 ± 0.1	2.5 ● 0.1	0.50 ± 0.02	0.26 ● 0.01
emission τ_e, μs	[a]	[a]	[a]	0.53 ± 0.02	0.25 ± 0.01

[a] Not observed. [b] Using the 532-nm excitation, a slower component of ~130 ps is also observed.

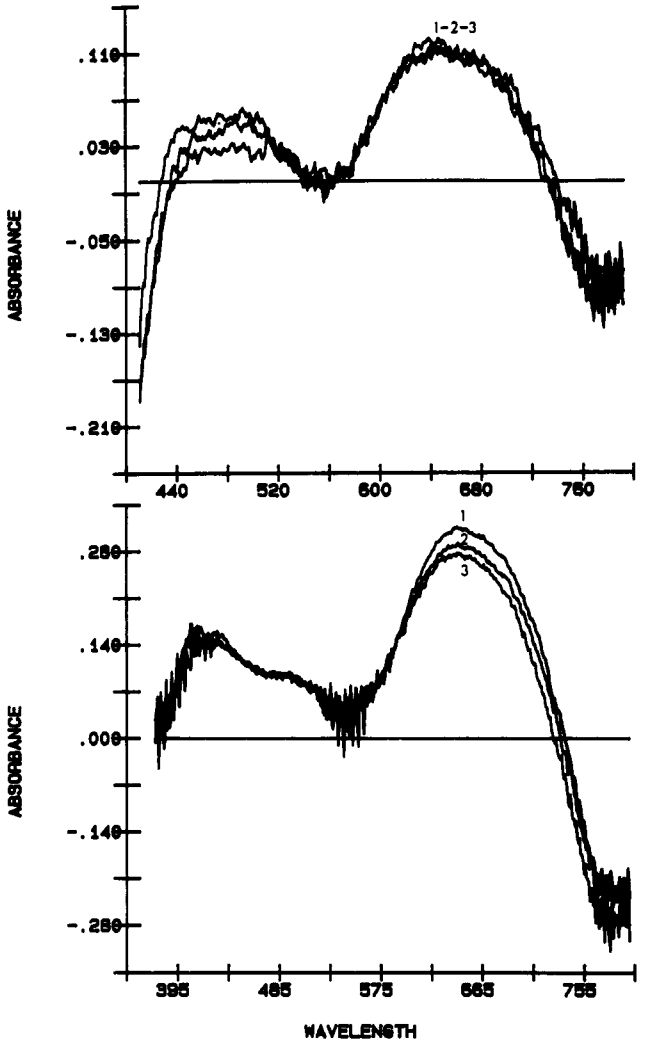

Figure 5. Difference absorption spectra of $Pt_2(dba)_3$ in toluene solutions at 298K using the 355- (top) and 532-nm (bottom) laser excitation at various delay times: (top) 1 = 140 ps, 2 = 2.1 ns, 3 = 4.8 ns; (bottom) 1 = 74 ps, 2 = 140 ps, 3 = 470 ps.

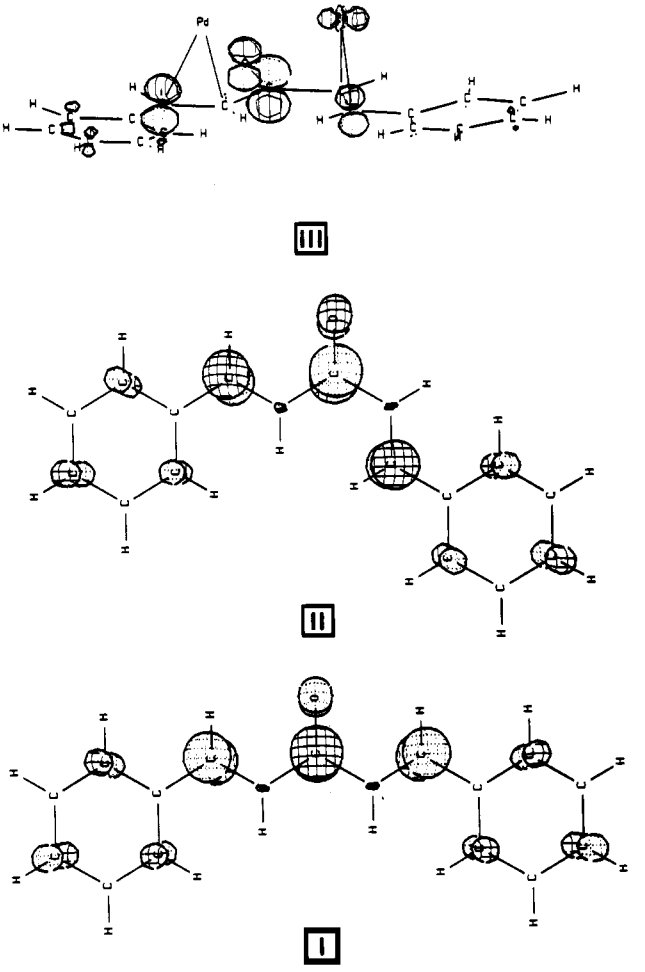

Figure 6. Comparison of the LUMO for dba in its s-cis,s-cis (I) and s-cis,s-trans (II) geometries (MO 42) and for dba in $Pd_2(dba)(CH_2{=}CH\text{-}(CO)CH{=}CH_2)_2$ (MO 78).

lowest energy singlet-state lifetime (as no fluorescence is detected for the $M_2(dba)_3$ complexes (M = Pd, Pt)). The Pd–olefin bond is particularly labile,[30] which makes the complexed dba capable of obtaining some degree of freedom (i.e. $Pd_2(\eta^4\text{-dba})_3 \rightleftarrows Pd_2(\eta^4\text{-dba})_2(\eta^2\text{-dba})$). We propose the assignment of the short-lived component in the excited $Pd_2(dba)_3$ complex to be a geometric isomer of the complexed dba. This efficient mechanism is completely reversible since no photoproduct is observed upon longtime broad band irradiation of $Pd_2(dba)_3$ in various solvents (toluene, halocarbons, THF) and in our flash photolysis experiments. The transient lifetime associated with the geometric isomer responsible for the cis-trans isomerization in free dba is 5.2 μs (in toluene at 294 K) and is significantly larger than the one measured for the complexed dba (in $Pd_2(dba)_3$)/toluene; 1.0 ns). This difference is consistent with the presence of interligand steric interactions in the complex and spin–orbit coupling (from the heavy Pd atoms) which contribute to deactivate transient and excited states. To further investigate this phenomenum ortho-substituted derivatives of dba could be used as bridging ligands where steric hindrance would be more important in the complexed form, potentially decreasing the 1.0-ns transient lifetime. Unfortunately, such complexes are relatively unstable at room temperature and long-term measurements (such as flash photolysis) appear rather difficult.[3b]

The $Pt_2(dba)_3$ difference absorption spectra (Figure 5) are very similar to that of $Pd_2(dba)_3$. The measured 0.25-μs lifetime (Table III) is in good agreement with the value measured previously in Me-THF (τ_e = 0.22 ± 0.01 μs)[2,3] based on emission measurements. Interestingly, no decay associated with the short component was observed, which could be consistent with the greater spin–orbit coupling effect of the heavier Pt atom and the much less labile Pt–olefin bond in $Pt_2(dba)_3$.[30] Table III summarizes the 298 K kinetic data for the investigated compounds in this work.

MO Calculations. Previous theoretical calculations on dba have shown that the s-cis,s-cis conformation is the most stable

(30) $Pd_2(dba)_3$ decomposes slowly in solution over days to form Pd(0) and free dba. $Pt_2(dba)_3$ is stable even after weeks in solutions.

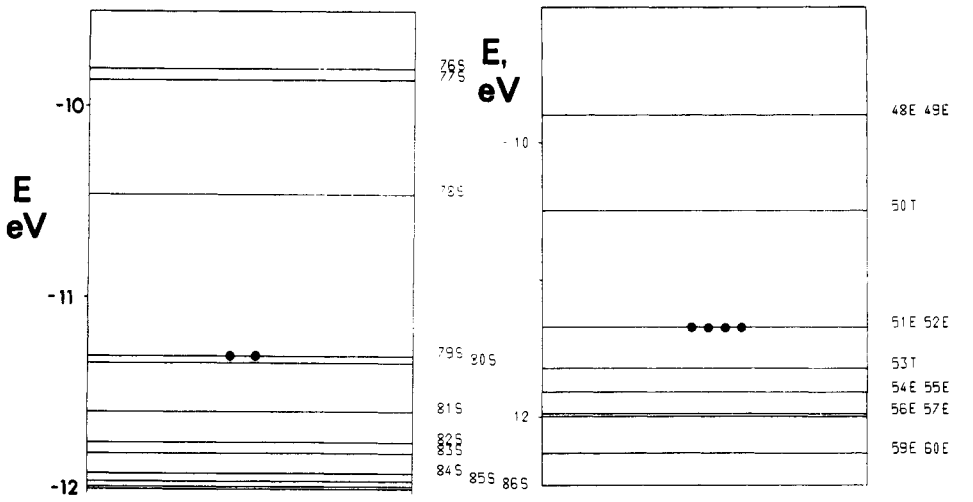

Figure 7. Partial MO diagram for $Pd_2(dba)(CH_2{=}CH(CO)CH{=}CH_2)_2$ (right) and $Pd_2(CH_2{=}CH(CO)CH{=}CH_2)_3$ (left).

one.[31] We have performed EHMO computations on both forms using the X-ray structure data for Medba and confirm these previous findings. Interestingly, MO energies near the LUMO and HOMO do not greatly change between the forms, and the atomic contributions to the MO's remain the same (Figure 6). The second feature of interest is the numerous MO's lying below the HOMO (within 0.6 eV) indicating that many IL dba states must lie nearby. We should note that the LUMO is well "isolated" from the upper MO.

To our knowledge there are no (rigorous or qualitative) theroetical studies on the $M_2(dba)_3$ compounds (M = Pd, Pt). In the mononuclear $Ni(C_2H_4)_3$ systems (D_{3h}; EHMO calculations),[32] the HOMO and LUMO are the 2e' and $1a_2''$ orbitals, which are primarily metal 3d and ethylene π^* in composition, respectively. Hence, the lowest energy electronic transition is MLCT (metal-to-ligand charge-transfer). In this work, EHMO calculations were performed on the model compounds $Pd_2(CH_2{=}CH(CO)CH{=}CH_2)_3$ and $Pd_2(dba)(CH_2{=}CH(CO)CH{=}CH_2)_2$ (all s-cis,s-trans conformation); the MO diagrams are shown in Figure 7. The HOMO and LUMO are labeled 78 and 79 (and perhaps the nearly degenerate 80 for $Pd_2(dba)(CH_2{=}CH(CO)CH{=}CH_2)_2$) and 50 and the degenerate 51 and 52 (for $Pd_2(CH_2{=}CH(CO)CH{=}CH_2)_3$), respectively, and are essentially metal 4d and dba π^* in character, respectively, and confirm the MLCT assignment for the $M_2(dba)_3$ compounds.[2-4] The LUMO for $Pd_2(dba)(CH_2{=}CH(CO)CH{=}CH_2)_2$ exhibits very similar atomic contributions to the dba LUMO particularly for the divinyl ketone moiety (Figure 6). The MO's 79–88 for $Pd_2(dba)(CH_2{=}CH(CO)CH{=}CH_2)_2$ and 51–60 for $Pd_2(CH_2{=}CH(CO)CH{=}CH_2)$ (4d metal) lie relatively nearby in energy, and more than one MLCT-type transition is possible. This observation is consistent with the presence of depolarization in the emission excitation spectra all along the MLCT region of the $Pd_2(dba)_3$ complex.[3] It is important to note that because both LUMO's for dba and the model compounds are very similar in nature, both the ILCT (for free dba) and MLCT (for $Pd_2(dba)_3$) states could exhibit similar chemistry. In this sense, the proposed assignment of the 1.0-ns species in the excited $Pd_2(dba)_3$ being a complexed dba geometric isomer appears to be supported by the MO analysis.

Acknowledgment. This research was supported by grants from the NSERC (Canada), the FCAR (Quebec), and the Université de Sherbrooke (Bureau de la recherche). P.D.H. thanks Dr. Davide M. Proserpio (Cornell University) for the help with the EHMO calculations.

Supplementary Material Available: Tables of atomic positional parameters, bond distances, bond angles, anisotropic thermal parameters, and collection parameters for Medba, tables of atomic orbital contributions of the MO's 48–60 for $Pd_2(CH_2{=}CH(CO)CH{=}CH_2)_3$ and 76–88 for $Pd_2(dba)(CH_2{=}CH(CO)CH{=}CH_2)_2$, and figures showing molecular geometries and numbering schemes (14 pages). Ordering information is given on any current masthead page.

(31) Tanaka, H.; Yamada, K.; Kawazura *J. Chem. Soc., Perkin Trans.* **1978**, *2*, 231.
(32) Rösch, N.; Hoffmann, R. *Inorg. Chem.* **1974**, *13*, 2656.